2009

Electrical activity and exocytotic correlates of biphasic insulin secretion from β-cells of canine islets of Langerhans

Stanley Misler
Washington University School of Medicine in St. Louis

Zhuan Zhou
Washington University School of Medicine in St. Louis

Adam S. Dickey
Washington University School of Medicine in St. Louis

Amelia M. Silva
Washington University School of Medicine in St. Louis

David M. Pressel
Washington University School of Medicine in St. Louis

See next page for additional authors

[Channels 3:3, 181-193; May/June 2009]; ©2009 Landes Bioscience

Research Paper

Electrical activity and exocytotic correlates of biphasic insulin secretion from β-cells of canine islets of Langerhans

Contribution of tuning two modes of Ca^{2+} entry-dependent exocytosis to two modes of glucose-induced electrical activity

Stanley Misler,[1,*] Zhuan Zhou,[1,2] Adam S. Dickey,[1,3] Amelia M. Silva,[1,4] David M. Pressel[1,5] and David W. Barnett[1,6]

[1]Departments of Medicine and Cell Biology; Washington University Medical Center; St. Louis, MO USA

[2]Current address: Institute of Molecular Medicine; Peking University; Beijing, China; [3]Current address: Medical Scientist Training Program; Pritzker School of Medicine; University of Chicago; Chicago, IL USA; [4]Current address: Department of Biology and Environment; CITAB; University of Trás-os-Montes e Alto Douro; Vila Real, Portugal; [5]Current address: Department of Pediatrics; A.I. duPont Hospital for Children; Wilmington, DE USA; [6]Current address: Department of Biomedical Engineering; St. Louis University; St. Louis, MO USA

Abbreviations: FPIS, first phase insulin secretion; SPIS, second phase insulin secretion; PSS, physiological salt solution; $[Ca^{2+}]_i$, cytosolic $[Ca^{2+}]$; I_{Ca}, voltage dependent Ca current; AP, action potential; PD, plateau depolarization; QREs, quantal release events; ΔC_m, membrane capacitance increase; $C_{m,\ step}$, step-wise increase in C_m after a depolarization; $C_{m,\ creep}$, progressive increase in C_m after a depolarization

Key words: biphasic insulin secretion, β-cell exocytosis, β-cell heterogeneity, phasic exocytosis, tonic exocytosis, membrane capacitance, amperometry

Biphasic insulin secretion in response to glucose, consisting of a transient first phase followed by a progressive second phase, is well described in pancreatic islets. Using single canine β-cells we have compared the time courses of electrical activity and insulin granule exocytosis to biphasic insulin secretion. Short trains of action potentials, similar those found during first phase insulin secretion, trigger phasic exocytosis from a small pool of insulin granules, likely an immediately releasable pool docked near voltage activated Ca^{2+} channels. In contrast, plateau depolarizations to between -35 and -20 mV resembling those during second phase insulin secretion, trigger tonic exocytosis from a larger pool of insulin granules, likely a highly Ca^{2+}-sensitive pool farther from Ca^{2+} channels. Both phasic and tonic modes of exocytosis are enhanced by glucose, via its metabolism. Hence, in canine β-cells two distinct components of exocytosis, tuned to two components of electrical activity, may contribute significantly to biphasic insulin secretion.

*Correspondence to: Stanley Misler; Renal Division/Medicine; Box 8126; Washington University Medical Center; St. Louis, MO 63110 USA; Tel.: 314.454.7719; Fax: 314.454.5126; Email: smisler@dom.wustl.edu

Submitted: 04/03/09; Revised: 05/08/09; Accepted: 05/11/09

Previously published online as a *Channels* E-publication:
http://www.landesbioscience.com/journals/channels/article/8972

Introduction

During a sustained rise in plasma glucose, pancreatic islets of Langerhans often display a biphasic time course of insulin release consisting of an initial, several minutes-long spike or first phase insulin secretion (FPIS), followed by a slowly developing but highly persistent dome or second phase insulin secretion (SPIS).[1,2] FPIS likely saturates insulin receptors on hepatocytes thereby blocking release of stored or newly formed glucose and stimulating importation of glucose newly absorbed from the intestinal tract. SPIS provides the sustained circulating concentrations of insulin needed to stimulate glucose uptake by peripheral adipocytes and by resting myocytes. In obese individuals, defects in biphasic secretion, coupled with target cell insulin insensitivity, contribute to the over-stimulation of the β-cell with eventual loss of secretory capacity.[3]

Biphasic insulin secretion has long been attributed to the existence of two pools of insulin granules in β-cells, namely a limited readily releasable pool (or RRP), discharged after a rapid rise in glucose and a larger, and more easily replenished, *reserve pool,* more slowly recruited for release.[4] There is now an emerging consensus that the pool responsible for FPIS, often called an immediately releasable pool (or IRP), requires local cytosolic $[Ca^{2+}]$ of tens of micromolar for discharge and is closely co-localized with (and docked at) voltage-dependent Ca^{2+} channels opened by early glucose-induced electrical activity.[5-7] However, the identity and the method of recruitment of the pool responsible for *SPIS* remain uncertain. Is this granule pool activated by (i) a slow-to-develop

glucose-derived signal perhaps large working independent of closure of ATP-sensitive K^+ (K^+_{ATP}) channels[8,9] or (ii) Ca^{2+} entry through a back-up voltage-dependent Ca^{2+} channel ($Ca_V2.3$), perhaps only activated during prolonged electrical activity?[10] Alternately, is the granule pool responsible for SPIS comprised of differently docked granules (e.g., lacking syntaxin) requiring a different spatio-temporal profile of activating [Ca^{2+}]?[11] Does this pool of granules correspond to the highly Ca^{2+} sensitive pool (HCSP), likely docked far from Ca^{2+} channels, sensitive to lower levels of local cytosolic [Ca^{2+}],[12] and proposed to account for exocytosis induced by prolonged depolarization in human and porcine β-cells.[13,14]

We have investigated depolarization-exocytosis coupling in patch-clamped single β-cells of dispersed canine islets of Langerhans using membrane capacitance (C_m) tracking[15,16] and amperometric measurements of quantal release of serotonin.[17,18] We now report that short trains of action potentials, (APs) similar to those seen during the brief FPIS,[19] trigger phasic (fast-on, fast-off) exocytosis from a small pool of insulin granules, likely corresponding to an IRP. In contrast, plateau depolarizations (PDs) to -35 to -20 mV, similar to those seen during prolonged SFIS,[19] trigger tonic (slow on-slow off and asynchronous) exocytosis from a larger pool of insulin granules, likely corresponding to the HCSP. Both phasic and tonic components of β-cell exocytosis are enhanced by glucose, whose metabolism appears to increase the sizes (and perhaps the refilling rates) of the underlying granule pools. On this basis we suggest that two components of exocytosis, tuned to the two components of electrical activity, may offer a relatively simple but novel model underlying biphasic insulin secretion in canine β-cells. Some of these results have previously been presented in abstract form.[20,21]

Results

Two phases of biphasic glucose-induced insulin secretion temporally correlate with two phases of biphasic glucose-induced electrical activity of β-cells of dispersed canine islets. Figure 1 presents the starting observations for our study. In A, note that when perifused at 32°C in the presence of 10 μM forskolin (closed symbols), aliquots of dog islets gently dispersed to a preparation of mostly single cells, respond to an increase in bath [glucose] from 3 to 12 mM with biphasic insulin secretion, although of slower kinetics, than those displayed by more intact canine islets perifused at 40°C in the presence of 10 μM forskolin (open symbols). The biphasic secretion consists of an initial FPIS, peaking 8–10 min after cells are first exposed to 12 mM glucose, followed by subsequent, slowly developing SPIS.

In B, note that under nearly identical ambient conditions (including similar constant perifusion), a single patch-clamped β-cell, representative of the majority (13/20) of cells recorded from, responds to an identical rise in bath [glucose] from 3 to 12 mM with biphasic depolarizing electrical activity. The first phase of electrical activity, lasting ~10 min is comprised of clusters (bursts) of large amplitude, brief action potentials (APs) at rates from 1–15 Hz, interrupted by brief intermittent plateau depolarizations. The second phase of electrical activity, persisting through the time course of development of SFIS, consists of a sustained plateau depolarization (PD), to between -35 and -20 mV. C, depicts the averaged time courses of spike activity and plateau depolarizations displayed by 5 of the 13 majority type responder cells. Note that during the first phase of electrical activity both the average number of APs/burst (or spikes/burst; upper trace), and the average number of bursts/min (middle trace) initially rise and then fall, while the percent of time the cell spends at a plateau potential positive to -35 mV (lower trace) increases progressively until the voltage-dependent Na^+ current inactivates and a sustained plateau depolarization develops.

Panels D and E demonstrate that FPIS and its temporally correlated interval of AP activity are both significantly depressed by tetrodotoxin (TTX), a blocker of voltage-dependent Na^+ channels, while the SPIS and its temporally correlated extended PD are significantly enhanced by BAYK 8644, an opener of L-type Ca^{2+} channels. Following exposure to 400 nM TTX, the first phase of insulin secretion is reduced by 45–60% while the frequency of simultaneously occurring APs is reduced by 80%. Following exposure to 10 μM BAYK 8644, the SPIS is increased nearly 4-fold while the amplitude of the simultaneously occurring PD is depolarized by 8–10 mV. In canine β-cells TTX inhibits whole-cell Na^+ currents at a K_i of 3.2 nM,[29] while BAYK 8644 negatively shifts the activation of whole-cell and single-channel Ca^{2+} currents (e.g. by 7 mV at 5–10 μM).[19]

Figure 1F shows aspects of the behavior of the minority of cells. The type I minority pattern, displayed by 3/19 cells, consists of an early transition from AP activity to a continuous PD then persisting throughout the remainder of the initial phase of insulin secretion. The type 2 minority pattern, displayed by 4/19 cells, consists of moderate frequency, lower amplitude AP activity persisting into the SPIS.

The strong temporal and pharmacological parallels between biphasic insulin secretion in dispersed, perifused islets and biphasic electrical activity in the majority of single β-cells suggests that the immediate stimulus for FPIS is intense Na^+-dependent action potential activity, while the stimulus for SPIS is the onset and persistence of the PD.

To better appreciate the patterns of electrical activity that support exocytosis we planned to monitor simultaneous electrical and amperometric activity of serotonin (5-HT) pre-loaded cells exposed to increased [glucose]. Unfortunately, 5-HT loaded β-cells depolarize poorly in response to glucose, much as they show blunted glucose-induced insulin secretion, a phenomenon reported for β-cells of other species.[30] While 5-HT-loaded cells depolarize in response to the sulphonylurea tolbutamide (e.g., Appendix Fig. 1D), the latter is a poor substitute for glucose, evoking only monophasic insulin secretion.[24,25] Therefore, we resorted to simulating the distinct phases of glucose-induced electrical activity and simultaneously monitoring the exocytosis in response to each phase.

Depolarization-induced exocytosis, tonic and phasic exocytosis. Figure 2 presents the two patterns of exocytosis displayed by single canine β-cells in response to brief trains of depolarizations to membrane potentials that evoke significant Ca^{2+} currents. They

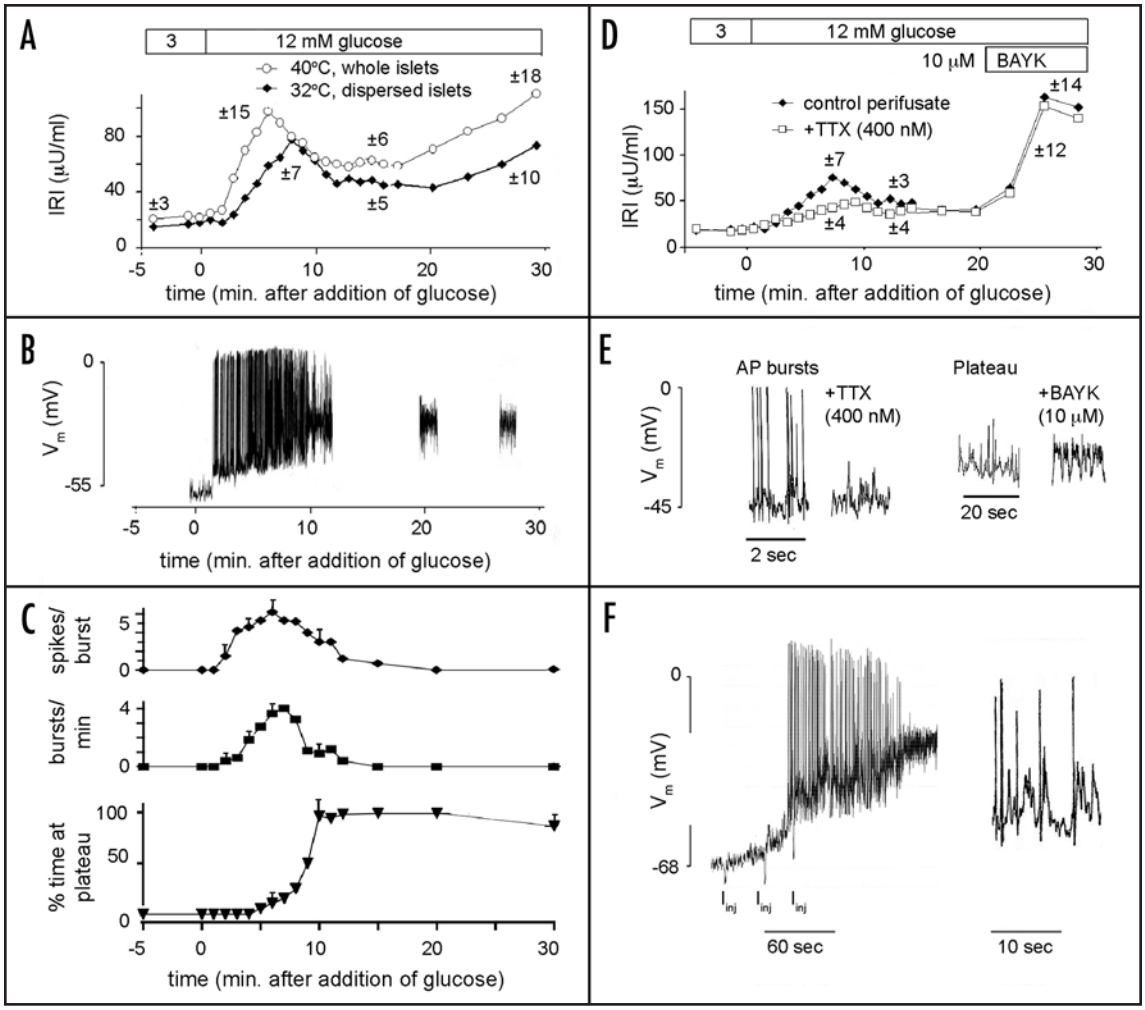

Figure 1. Correlation of biphasic insulin secretion with biphasic electrical activity in β-cells of dispersed canine islets of Langerhans. (A) in the presence of 10 μM forskolin, increasing the perifusate [glucose] from 3 to 12 mM evokes biphasic insulin secretion from dispersed islets (◆) at 32°C, as well as from whole islets (○) at 40°C. In both conditions an initial spike-like FPIS is followed by the transition to a slowly increasing dome-like SPIS, though in dispersed islets perifused at the lower temperature both the time-to-peak of the spike and subsequent transition to dome phase are delayed by several minutes. (B) at 32°C in the presence of 10 μM forskolin, increasing the [glucose] from 3 to 12 mM evokes biphasic electrical activity from single patch-clamped β-cells. With similar time course as FPIS, there is an initial phase of accelerating AP frequency accompanied by slower development of intermittent plateau depolarizations; with similar time course as the transition to the dome phase of insulin secretion, a steady PD develops. (C) averaged time courses of development of AP activity and PD in five cells after increasing [glucose] of the perifusate from 3 to 12 mM. Note that during the first 10–12 min in 12 mM glucose the intensity of AP activity, characterized by bursts of up to 5 APs/burst (upper trace) and up to 5 bursts/min (middle trace), initially increased and then decreased (lower trace), while the fraction of time the cells spent at the PD progressively increased until the APs inactivated and a sustained PD developed. After several minutes into the sustained PD, V_m sometimes displayed transient repolarizations which reduced its average value by several mV. (D and E) parallel effects of TTX and BAYK 8644 on insulin secretion (D) and electrical activity (E). TTX reduced FPIS and blocked the development of bursts AP; BAYK 8644 raised SPIS as well as average amplitude of the PD. (F) electrical activity of two minority type cells. Left, rapid transition from AP activity to PD based on closure of K^+_{ATP} channels, the latter indicated by increasing membrane hyperpolarization to current injection pulses, I_{inj}, of -5 pA. Right, AP activity persisting for 25 min in 12 mM glucose.

suggest that there are two components of depolarization-induced exocytosis. In experiments of the type illustrated in panels A and B, increases in the membrane capacitance (C_m) of a β-cell were measured in response to trains of three depolarizing pulses, each of 25 or 50, 100 or 200 ms duration, applied at 1 Hz to +5 mV, where I_{Ca} is maximal (viz. Appendix Fig. 1B). Trains of depolarization were limited to three pulses separated by 3-minute intervals, to reduce the rapid granule depletion and contamination of traces by any slow component of endocytosis. In *A*, representative of 11/25 cells, note that the first depolarization, up to 200 ms in duration, fails to trigger a measurable increase in C_m, in spite of evoking peak Ca^{2+} currents (I_{Ca}) ~-150 pA. However, repeated 50 and 100 ms depolarizations evoke slow but progressive increases (or "creeps") in C_m (abbreviated as $C_{m,\,creep}$) during the interpulse interval and often continuing for 2–5 s after the depolarizing train ended. We call this delayed and sustained (i.e., "slow-to-start, slow-to-stop") pattern of C_m increase tonic (or steady and asynchronous) exocytosis.

In contrast, in B, representative 14/25 cells, brief 50 ms depolarizations, each evoking a peak I_{Ca} of -140 pA, were sufficient to

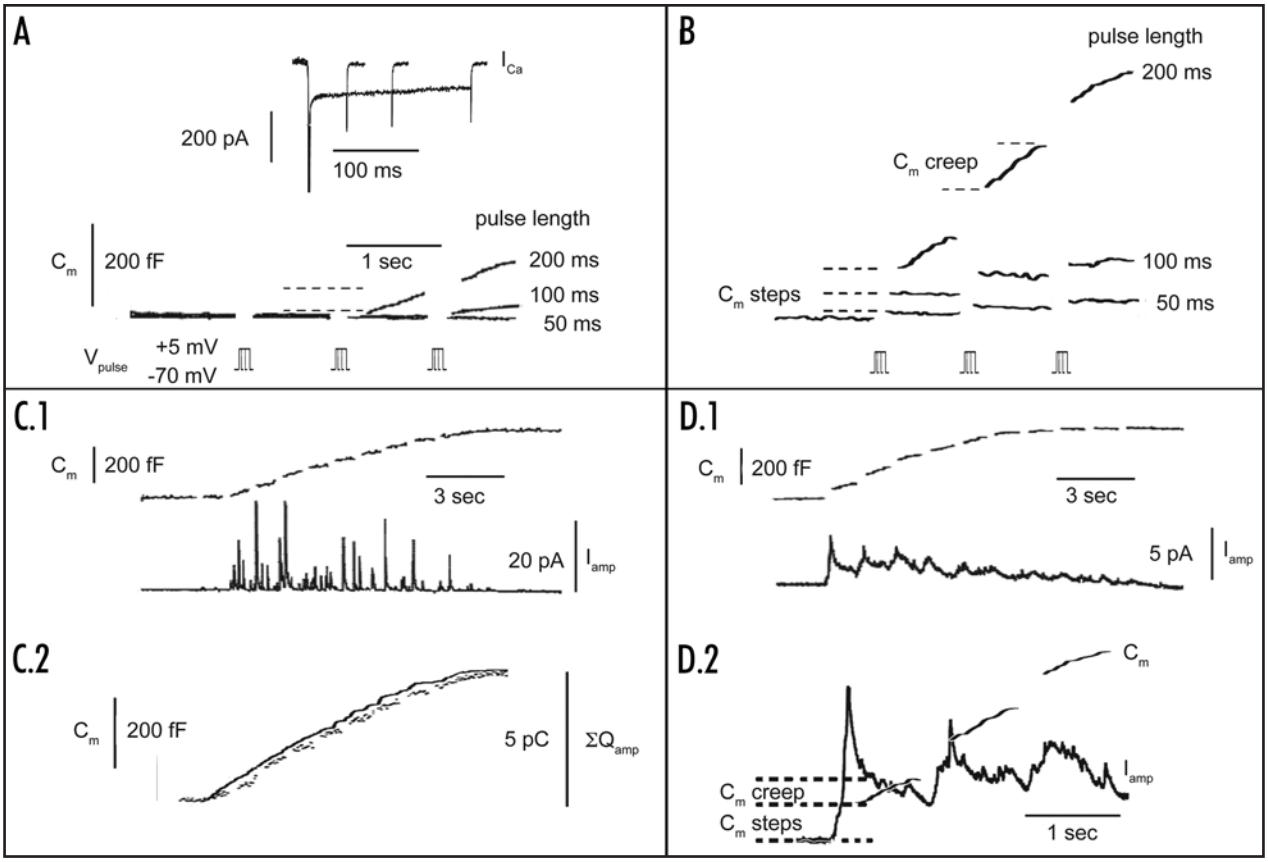

Figure 2. Modes of exocytosis in canine β-cells monitored by increases in membrane capacitance (C_m) and the frequency of quantal release events (QREs). (A and B) contrast two patterns of exocytosis: tonic (or asynchronous and sustained) exocytosis vs. phasic + tonic (or synchronous and transient + asynchronous and sustained) exocytosis. In (A), where no step-wise increase of C_m was seen in response to the first depolarizations, tonic exocytosis, manifested as post-stimulus continuous increase in C_m (denoted as $C_{m,\ creep}$), were first triggered by the second 200 ms depolarization, or the third 100 ms depolarization, to +5 mV. Top inset shows sample current traces evoked by 50, 100 and 200 ms pulses. In (B), phasic exocytosis was seen as a $C_{m,\ step}$ triggered by a single 50 ms depolarization, but its amplitude increased after more extended (100 and 200 ms) depolarizations. In this cell with phasic + tonic exocytosis, $C_{m,\ creeps}$ were seen after the second and third 200 ms depolarizations. (C and D) exocytosis monitored simultaneously as C_m increases and increased frequencies of QREs. In the case of tonic exocytosis shown here (C), the first depolarization failed to evoke exocytosis while subsequent depolarizations in the train evoked a progressive C_m creep and an increasing frequency of QREs (see C,1). The overlay of scaled traces of C_m and Q_{amp} (the running integral of I_{amp}) demonstrates the close temporal correspondence of two measures of exocytosis, including the exhaustion of exocytosis by the final depolarization of the train (C,2). With phasic + tonic exocytosis (D), the large steps in C_m, seen immediately after a depolarizing pulse, correspond well to the burst of QREs during the breaks in the C_m traces representing the stimulus interval. (D,2) expanded from (D,1).

trigger a small but reliably detectable "step" in C_m (abbreviated as $C_{m,\ step}$), while long (200 ms) depolarizations, each evoking a larger Q_{Ca}s, triggered larger $C_{m,\ step}$s, followed by a prolonged $C_{m,\ creep}$. However, during a train of 200 ms depolarizations, with each successive depolarization the amplitude of the $C_{m,\ step}$ declined even as the slope of the $C_{m,\ creep}$ increased. We call this "rapid-to-start" pattern of C_m increase, which transforms into a "slow-to-stop" pattern, phasic (or synchronous and transient) exocytosis + tonic (or asynchronous and sustained) exocytosis.

C and D, present simultaneous capacitance and the amperometric recordings of tonic and phasic + tonic patterns of exocytosis, respectively, in two β-cells preloaded with 5-HT and subjected to trains of ten 200 ms depolarizations to +10 mV. In each case note the similar time courses of exocytosis seen with both assays. In C,1, note the absences of both quantal release events (QREs) and capacitance increases (ΔC_ms) after the first depolarizing pulse, as compared with (ii) the increasing frequency of QREs paralleling the steadily developing $C_{m,\ creeps}$ in the inter-pulse intervals beginning after the second depolarizing pulse and continuing through several subsequent 200 ms depolarizations. The close correlation of the time courses of C_m and the occurrence of QREs is further displayed in C,2, where the C_m trace overlays a scaled running sum of amperometric charge (ΣQ_{amp} = running integral of the amperometric current). These data suggest that both assays are measuring exocytosis evoked from the same pool of granules. The subsequent 'trail off" of both assays of exocytosis with repetitive depolarization may reflect the onset of endocytosis at a time when the release-ready granule pool components are being depleted. In contrast, in D,1, where $C_{m,\ steps}$ are clearly noticeable immediately after each of the first three depolarizations, note the bursts of amperometric current, representing overlapping QREs, during each depolarization, as well as the tails of other overlapping QREs persisting into the inter-pulse interval and coinciding with the $C_{m,\ creeps}$ (see overlay of expanded traces of C_m and I_{amp} in D2). During the train of depolarizations,

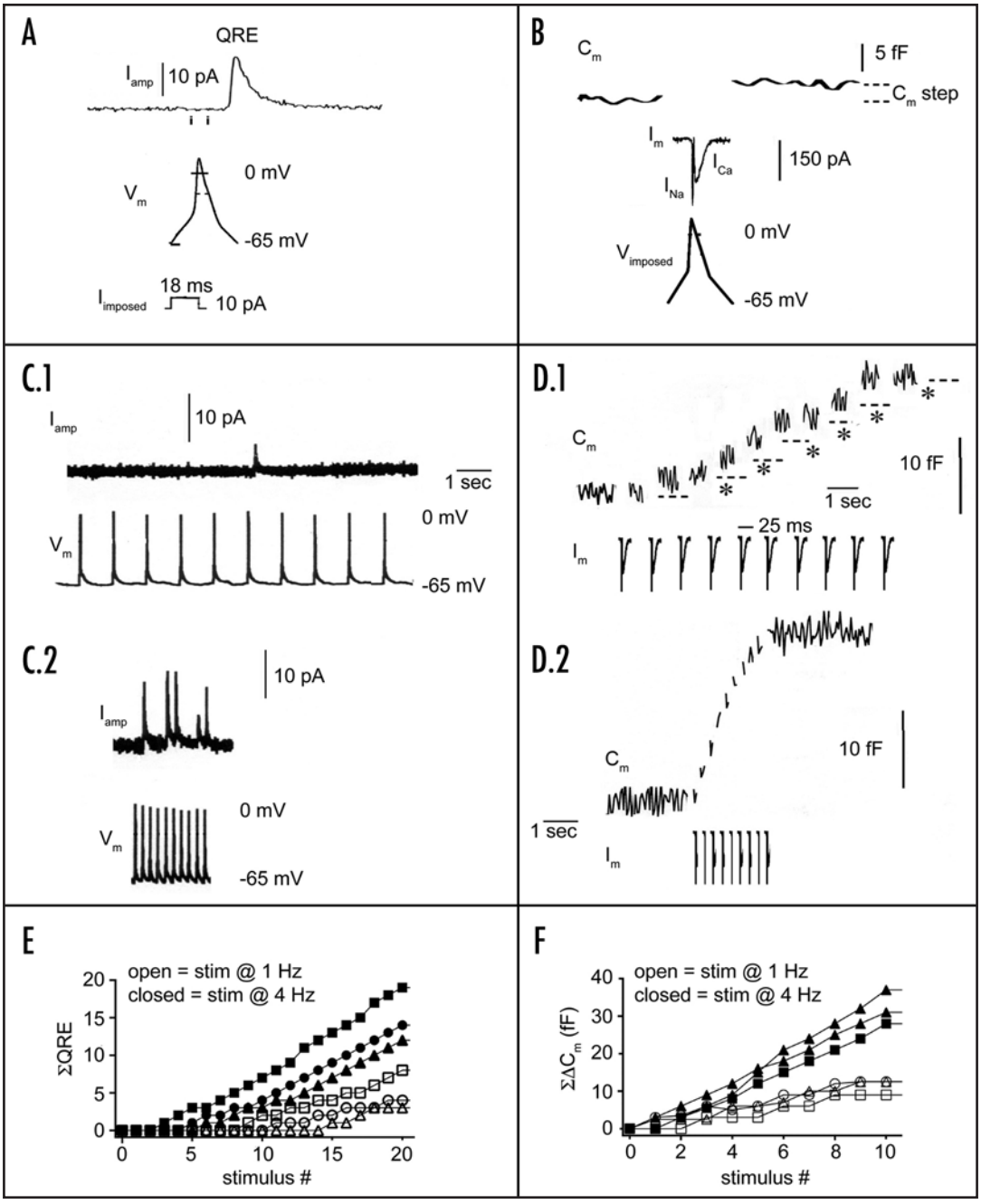

Figure 3. Examination of phasic exocytosis in response to action potential activity evoked by current injection (A, C and E) and action potential simulation under voltage-clamping (B, D and F). (A) demonstrates that in selected cells stimulated at 0.2 Hz, brief depolarizing current pulses (10 pA), producing rapid upstroke action potentials with overshoots to +10 mV, provoked an occasional QRE within 25 ms. (B) demonstrates that in selected cells, here stimulated at 0.2 Hz, single simulated APs of similar morphology as in A (and producing a rapid I_{Na} followed by a slower developing I_{Ca}), provoke $C_{m,\ steps}$ seen immediately after the termination of the complex depolarizing pulse. (C) demonstrates, in cells poorly responsive to stimulation at 0.2 Hz, that increasing the frequency of depolarization-evoked APs from 1 Hz (C,1) to 4 Hz (C,2) increases quantal release efficiency by several-fold. Similarly (D) demonstrates that increasing the frequency of voltage-clamp simulated APs from 1 Hz (D,1) to 4 Hz (D,2) enhances the total C_m increase by nearly 3-fold. In (D,1) note discrete measureable $C_{m,\ steps}$ (marked by *s) after depolarizing pulses numbers 2, 4, 5, 6, 8 and 9. (E and F) present comparisons of cumulative exocytosis in response to trains at 4 Hz vs. 1 Hz, using each of the two experimental paradigms shown in (C and D).

both the tonic and phasic components of exocytosis undergo significant depletion, though depletion of the phasic component appears to be faster. We shall return to this point later.

Phasic component of exocytosis occurs during brief bursts of action potentials. Assuming that early electrical activity constitutes the basis for FPIS, then single APs or short burst of APs occurring at a frequency of 1–4 Hz should support single cell *phasic* exocytosis. In Figure 3 we demonstrate that single or short trains of APs, evoked by brief depolarizing current pulses, trigger QREs, while voltage waveforms simulating APs trigger small C_m steps.

In *A,* depicting data from a particularly robustly secreting cell stimulated at 0.2 Hz, note that a single AP evoked by a brief 18 ms injection of current (10 pA) results in a QRE after a latency of 25–50 ms. In B, obtained from a similar robustly secreting cell stimulated at 0.2 Hz, a simulated AP, of waveform similar to the AP recorded in A, and evoking a rapidly inactivating I_{Na} followed by slowly deactivating I_{Ca} (Appendix Fig. 1C for details), results in a small step in C_m ~ 3.5 fF. (For the 50 responses recorded in response to 120 trials step size ranged from 2–4 fF, or roughly equivalent to the 2–2.5 fF step size expected from the exocytosis of a 250–300 nm diameter secretory granule, given the intrinsic noise even of filtered records and the resolution limits of the recording system). The probability of recording a QRE in response to an isolated evoked AP on average was significantly lower at ~10–15%, probably due to the limited area of cell surface available to the amperometric electrode. All QREs had a latency (time from peak of AP to peak of QRE) of <100 ms.

In contrast, in other cells, brief trains of 10–20 APs, evoked at frequencies between 1 an 4 Hz, were quite effective at eliciting QREs and measurable changes in C_m, even though isolated APs evoked at 0.2 Hz were not. Strikingly, in response to APs applied at a frequency of 4 Hz, the number of QREs recorded during the train was on average of 3.6-fold larger than at 1 Hz (compare traces in C,2 with C,1). In addition, the latency of the QREs was wider at 4 than at 1 Hz, with only 70% of events occurring within 100 ms at 4 Hz vs. 85% at 1 Hz; this likely reflects the development of tonic or asynchronous release with prolonged stimulation. Similarly, in response to simulated APs applied at 4 Hz, the total ΔC_m by the train was augmented by 2.6-fold over that seen in response to simulated APs at 1 Hz (compare traces in D,2 with D,1). Consistently, the first AP of the train was not effective in evoking release while later APs became increasingly effective in doing so. Summary data for this effect are shown in panels E and F. The "tuning" of exocytosis to bursts of several APs, as opposed to single isolated APs, suggests that a causal link might underlay the temporal correlation of increasing release during FPIS with the ongoing increase AP activity (APs/burst and bursts/min). The increasing efficiency of exocytosis during the much of the course of an AP train suggests facilitation of release due to Ca^{2+}-dependent priming of the exocytotic process.

Tonic component of exocytosis operates over the range of plateau phase depolarizations and is sustained by a rise in global $[Ca^{2+}]_i$ to >500 nM. If a prolonged plateau depolarization in the range of -30 to -20 mV constituted the basis for plateau phase secretion, then voltage-clamp depolarizations into this range should sustained exocytosis. Figure 4 investigates the voltage-dependence and the timing of quantal release during and after brief trains or continuous depolarizations in an attempt to relate tonic exocytosis to prolonged Ca^{2+} entry and the resultant rise in global $[Ca^{2+}]_i$. A, compares the exocytotic efficiencies of 5 s long depolarizations to different V_c values in a cell that we had previously shown to require at least 200 ms of continuous depolarization to initiate exocytosis. Each depolarization was followed by a rest period of 90–120 s at -70 mV to insure recovery from depletion of the store of readily releasable exocytotic granules. While a depolarization to -35 mV, evoking a total Ca^{2+} entry of 1.6 pC, produced no detectable exocytosis detectable, depolarizations to -30, -20 and -10 mV, which evoked progressively larger Ca^{2+} entries (4.2, 8.7 and 25.4 pC; respectively), were increasingly effective in triggering quantal release, beginning after briefer delays during the prolonged depolarization, and continuing for up to several seconds after cessation of the depolarization. Of physiological importance is the steep increase in depolarization-induced exocytosis over the range of -35 to -20 mV range, the pertinent voltage range for glucose-induced plateau depolarizations.

The features of long latencies to onset of depolarization-induced exocytosis and ongoing exocytosis after cessation of Ca^{2+} entry displayed by the cell in panel A suggests that a threshold of Ca^{2+} entry and cytosolic Ca^{2+} accumulation must be exceeded prior to the onset of secretion and that secretion continues until cytosolic Ca^{2+} falls below that threshold. We investigated some of these features in more quantitatively in three cells, in which Ca^{2+} currents showed very slow inactivation and individual amperometric events showed little overlap. These cells were depolarized, in random order to -35, -30, -20, -10 mV. In panel B, for each cell the running sum of the number of amperometric spike events (ΣASE) was plotted against total Ca^{2+} entry (ΣQ_{Ca}) at each depolarizing voltage. Each cell had an apparent "threshold" value of Q_{Ca}, ranging from 4–5 pC to 10–12 pC.

We hypothesized that the tonic exocytosis displayed in response to repetitive or prolonged depolarization resulted from slow build-up of the global $[Ca^{2+}]_i$, to levels that triggered exocytosis, followed, after Ca^{2+} entry ceased, by the subsequent decline in $[Ca^{2+}]_i$, and disappearance of the exocytotic response. The threshold dependence on Ca^{2+} entry would then represent the interaction of voltage-dependent Ca^{2+} entry and the properties of cytosolic and organelle-based Ca^{2+} buffers, to convert plasma membrane Ca^{2+} entry into uniform elevation of free $[Ca^{2+}]_i$ available to trigger release. To test this hypothesis we used patch-clamped β-cells that appeared uniformly fluorescent after loading with Fura-2 to examine, during a train of repetitive depolarizations, the relationship of the development of $C_{m,\ creep}$ to the monitored rise in $[Ca^{2+}]_i$. Cells chosen for analysis displayed little to no $C_{m,\ step}$ after a single 200 ms depolarizing pulse to +5 or +10 mV and little decline in C_m over the 5–10 s following the train. Depolarizing pulses of 200 ms duration were applied in attempt to obtain uniform elevation of Ca^{2+} concentration during each pulse as is possible with adrenal chromaffin cells.[31]

Using the Fura-2 fluorescence ratio (F_{340}/F_{380}) as an indicator of free cytosolic $[Ca^{2+}]$, $[Ca^{2+}]_i$, Figure 4C demonstrates the parallel rises in rate of $C_{m,\ creep}$ and $[Ca^{2+}]_i$, from the third depolarization through to 1–2 s after the last 5th depolarization. Thereafter, the rate of $C_{m,\ creep}$ declines in tandem with a drop in Fura-2 fluorescence ratio. To quantify this, the C_m trace from the end of the 3rd depolarization through following 15 s was fit to a high order polynomial in an attempt to both smooth the data and interpolate between the gaps created during depolarizations. This polynomial was differentiated to produce the trace labeled dC_m/dt, which was taken to represent $C_{m,\ creep}$. *D*, shows a set of these derived traces, plotted against calibrated $[Ca^{2+}]_i$, for three separate experiments. The dC_m/dt increased as a supralinear function of $[Ca^{2+}]_i$ over the $[Ca^{2+}]_i$ range of 500 to 1,000 nM. Importantly,

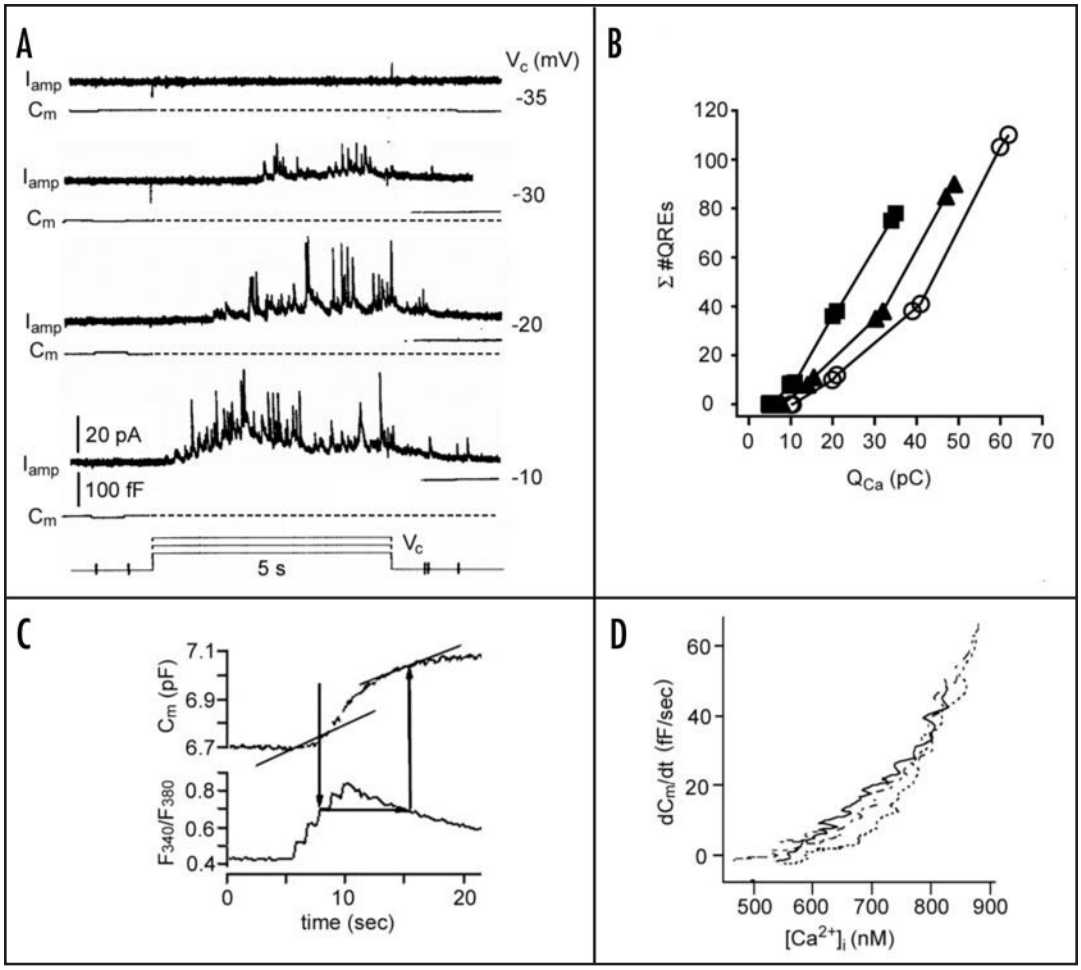

Figure 4. Prolonged depolarizations to values of V_m resembling glucose-instigated PDs evoke Ca^{2+} entry-dependent exocytosis. (A) combined measurement of I_{amp} and C_m, during and again after 5 s depolarizations to V_c = -35, -30, -20 and -10 mV. Note that with depolarizations to more positive V_c values, where total depolarization-evoked Ca^{2+} charge entry (Q_{Ca} = integral of I_{Ca}) increases, both the number of QREs and post-pulse ΔC_m increase, while the latency to the occurrence of the initial several QREs shortens. (B) relationship of exocytosis, measured by the running sum of QRE, to Q_{Ca} in the three most stable cells, where at least two depolarizations, either to -35, -30, -20 or -10 mV, were applied in random order at 90 s intervals. (See text for more details). (C) simultaneous recording of C_m (upper trace) and Ca^{2+} fluorescence ratio (F_{340}/F_{380}) in a Fura-2 pre-loaded cell. A train of five 200 ms depolarizations to 0 mV was applied at 1 Hz. (D) correlation of the rate of $C_{m,\ creep}$ (dC_m/dt) with calibrated cytosolic calcium concentration, $[Ca^{2+}]_i$, from experiments similar to that shown on *C* (see text for details).

this is the minimum range of $[Ca^{2+}]_i$ needed to induce the slow rates of continuous exocytosis in β-cells seen either in cells dialyzed via whole-cell patching with pipettes containing buffered Ca^{2+} solutions[32] or permeabilized to extracellular Ca^{2+} by the channel-forming neurotoxin α-latrotoxin.[33] In addition, it is the minimum range of $[Ca^{2+}]_i$ that induces slow rates of insulin secretion from perifused β-cells previously permeabilized with digitonin.[34]

Phasic and tonic components of exocytosis are enhanced, over minutes, by concentrations of extracellular glucose that trigger biphasic insulin secretion. In correlating electrical activity with insulin secretion it appeared that AP activity peaked earlier than the peak of FPIS, while average plateau depolarization sagged by 2–3 mV, likely due to some long term Ca^{2+} channel inactivation, even as SPIS was increasing. This suggested that in the presence of secretogogue levels of glucose, over minutes, some factor(s) might be contributing to a progressive increase in the efficiency of depolarization-exocytosis coupling. In an initial approach we tested whether glucose and glucose metabolism might be such a factor.

Figure 5 demonstrates that raising extracellular glucose concentration, into the range that produced biphasic insulin secretion, enhanced both phasic exocytosis, proposed to predominate during the time course of FPIS, as well as tonic exocytosis, proposed to begin during first phase secretion and grow to be predominant during SPIS. In a sample cell (Fig. 5A), in the presence of 4 mM glucose, five 50 ms depolarizations to 0 mV applied at 1 Hz produced steps of C_m exclusively. However, after 10 min exposure to 12 mM glucose, the first two depolarizations produced larger C_m steps while the subsequent depolarizations evoked C_m creeps. After 25 min in 12 mM glucose there appeared to be no further enhancement of $C_{m,\ steps}$ while $C_{m,\ creeps}$ were enhanced and were in evidence after earlier depolarizations. All of this occurred in the face of a modest (12%) *decrease* in Ca^{2+} entry, suggesting profound augmentation of the processes underlying both phasic and tonic exocytosis, perhaps through an increase in the pool of readily

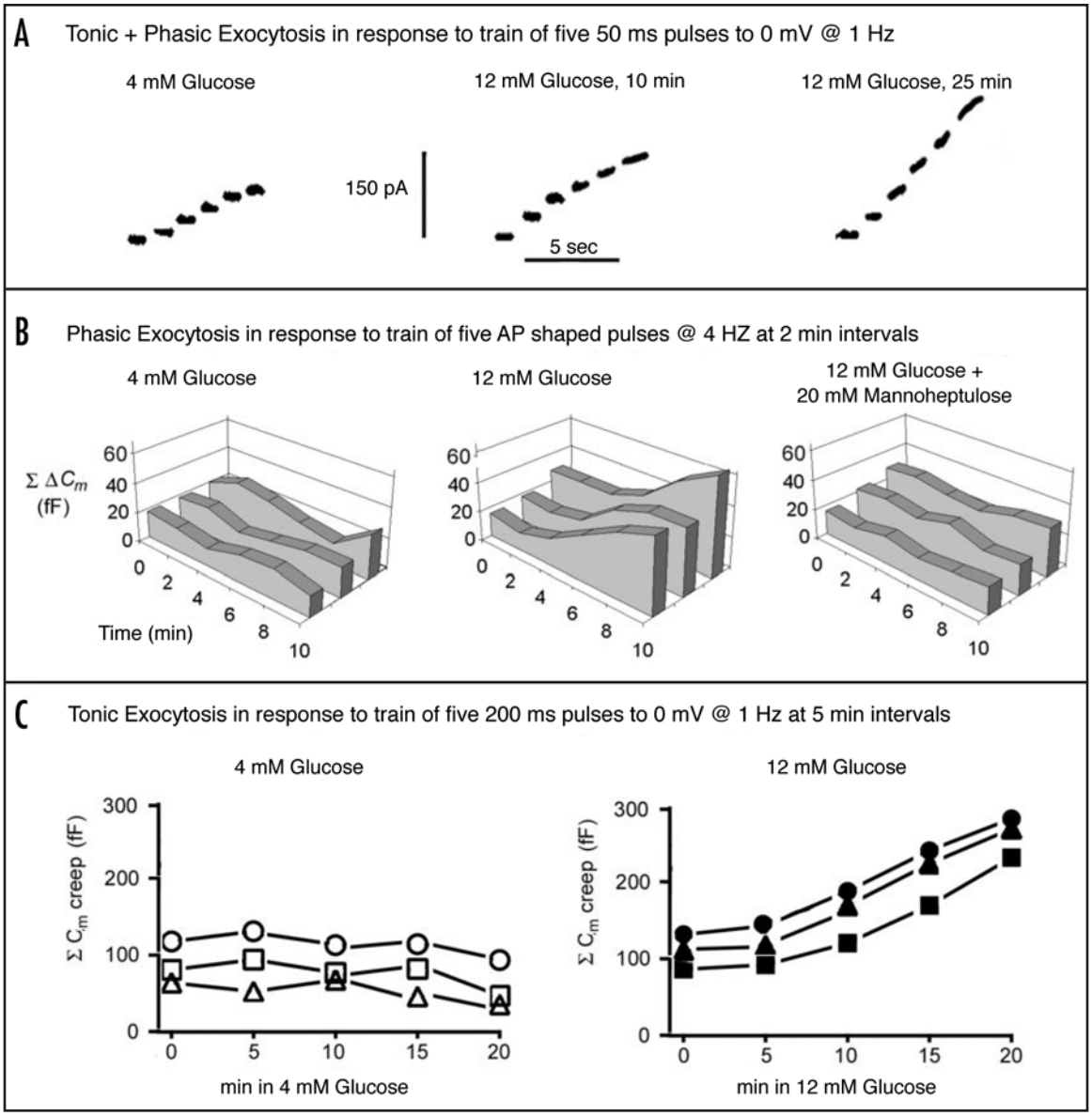

Figure 5. Progressive enhancement of phasic and tonic exocytosis during prolonged exposure to concentrations of glucose that promote insulin secretion. (A) overview of the effects of glucose on both modes of exocytosis from single canine β-cells. *Left*, control cell displaying very clear phasic exocytosis in response to a train of five 50 ms pulses to 0 mV applied at 1 Hz in 4 mM glucose. *Middle*, same cell after 10 min exposure of cell to 12 mM glucose; note the enhancement of $C_{m,\ steps}$, in response to the first two depolarizations, and modest development of $C_{m,\ creep}$, in response to depolarizations 3 to 5. *Right*, same cell after 25 min exposure to 12 mM glucose; note the stable enhancement of $C_{m,\ steps}$, in response to the first two depolarizations, and further development of $C_{m,\ creep}$. (B) effects of glucose and glucose metabolism on the time course of phasic exocytosis evoked by a train of 10 standard AP-shaped pulses (identical to those used in Fig. 3B) applied at 4 Hz once every 2 min. Note that the progressive increase in train-evoked $C_{m,\ steps}$ over 10 min in 12 mM glucose vs. the stable pattern of $C_{m,\ steps}$ in 4 mM glucose. Also the effect of elevated glucose is abolished by addition of mannoheptulose, an inhibitor of phosphorylation of glucose after its entry into the cytosol. (C) effects of glucose on the time course of development of tonic exocytosis, measured as summed $C_{m,\ creep}$ in response to a train of five 200 ms pulses to 0 mV, delivered at 1 Hz, at five min intervals. Note the slow increase in summed $C_{m,\ creep}$ beginning by 10 min of exposure to 12 mM glucose, as compared with the stable response pattern in 4 mM glucose.

releasable granules.

We further examined the effect of glucose exposure on depolarization-exocytosis coupling in the face of stimuli more closely simulating glucose-induced electrical activity. To investigate the effects of glucose and glucose metabolism on phasic exocytosis, in B we measured C_m increase ($\Sigma\Delta C_m$), consisting almost exclusively of steps of C_m, in response to a train of ten simulated APs applied at 4 Hz every 2 min to cells maintained under three distinct conditions. While in 4 mM glucose $\Sigma\Delta C_m$ remained constant over 10 min, in 12 mM glucose $\Sigma\Delta C_m$ progressively increased up to 2.5 fold. In contrast, in the presence of 12 mM glucose + 20 mM mannoheptulose, an inhibitor of the cytoplasmic phosphorylation of transported glucose, $\Sigma\Delta C_m$ was again stable over the 10 min. To investigate the effects of glucose and glucose metabolism on tonic

exocytosis, in C we measured the effect of 4 vs. 12 mM glucose on the time course of development of $C_{m,\ creep}$ during a train of five 200 ms depolarizations to 0 mV applied at 1 Hz. When test trains were applied every 5 min to 3 cells exposed to 4 vs 12 mM glucose, note that in 4 mM glucose the total $C_{m,\ creep}$ per train (or $\Sigma\Delta C_{m,\ creep}$) remained constant over 10–15 min but then tended to decline. However in 12 mM glucose $\Sigma\Delta C_{m,\ creep}$ increased progressively increased by up to 3 fold over 20 min, this in spite of an average a progressive decrease peak in I_{Ca} and Q_{Ca} of up to 15% by 20 min, which would otherwise depress exocytosis by at least 30%.

Discussion

Biphasic insulin secretion in response to a sustained rise in glucose to above 10 mM is common to islets of many mammalian species. Several hypotheses have been proposed to account for it. In this paper we explore its exocytotic correlates in single canine β-cells and suggest that tuning two modes of exocytosis (phasic and tonic) to two modes of glucose-induced electrical activity (action potential trains and plateau depolarizations, respectively) is a major contributor to biphasic insulin secretion in the dog.

Under nearly identical conditions of stable ambient temperature of 32°C and forskolin, individual canine β-cells display biphasic glucose-induced insulin secretion that temporally and pharmacologically closely parallels biphasic electrical activity. FPIS, which is suppressed TTX, is concurrent with increasing intensity of bursts of Na^+_o-dependent APs, reaching a peak intensity of nearly 5 APs/burst and 4 bursts/min. The transition to SPIS is concurrent with the waning of AP activity and the development of a prolonged PD between -30 and -25 mV, with both SPIS and PD enhanced by BAY K 8644. Furthermore, under identical conditions we have also monitored single cell exocytosis using two real-time assays. Consistently, we find that the two patterns of electrical activity clearly evoke two components of exocytosis from canine β-cells. Evoked or simulated APs, clustered at 1 to 4 per second, largely evoke a *phasic* component of exocytosis, consisting of single QREs and small steps C_m, well-synchronized with (i.e., during, or within 50 ms of termination of) the evoked or simulated AP. In contrast, PDs evoke a *tonic* component of exocytosis, consisting of barrages of QREs or continuous increases in C_m beginning up to hundreds of ms after the start of a depolarization and continuing for up to several seconds after its conclusion. The near synchrony of occurrence of QREs and C_m increases (within the 25–50 ms limit of resolution of the post-stimulus measurement of C_m) suggests that both assays reflect the same basic exocytotic process.

Quantitatively, the vast majority of canine β-cells respond within 2–4 minutes of a rise in [glucose] from 3 to 12 mM by firing short trains of large amplitude APs; more than half of these cells undergo exocytosis in response to single or short trains of AP-like depolarizations. On this basis we suggest that moderate frequency AP activity, leading to a "phasic" component of exocytosis, may be the basis for FPIS. In addition, the vast majority of canine β-cells respond within 12 min with PDs to -30 to -25 mV and begin to exocytose within <500 ms after onset of such PDs. On this basis we suggest that PDs resulting in tonic component exocytosis may be the basis for SPIS. Both phasic and tonic components of exocytosis are enhanced at concentrations of ambient glucose that provoke insulin secretion. In the presence of 12 mM glucose, the potency of the phasic component of exocytosis is increased 2–3 fold over the time course of first phase insulin secretion; this likely ameliorates any depression of release that might result from moderately declining intensity of AP activity after an early peak. Similarly, the potency of the tonic component of exocytosis is similarly increased throughout the early segment of dome phase of insulin secretion, even as the sustained PD sags by several mV. Hence, provided that our assays of exocytosis adequately reflect insulin secretion, the combination of the two components of exocytosis, tuned to release by distinct modes of electrical activity, plus the effects of glucose on each, may be sufficient to account for a large portion of biphasic insulin secretion in isolated canine β-cells.

Mechanistically, by analogy to previous work done on mouse β-cells and INS-1 clonal insulinoma cells, it is likely that granule pools underlying the phasic vs tonic components of exocytosis differ in their Ca^{2+} sensitivities for fusion, and their localization with respect to plasma membrane Ca^{2+} channels.[12] We propose that phasic exocytosis evoked by single or short trains of single APs occurs from an immediately releasable pool (or IRP) closely co-localized with high voltage-activated (HVA) and likely L-type Ca^{2+} channels; granules in this pool experience micro-domains of cytosolic [Ca^{2+}] in the tens of μM and display low Ca^{2+} sensitivity (>5 μM). In addition, we propose that tonic exocytosis evoked by prolonged plateau results from a highly Ca^{2+} sensitive pool (HCSP) poorly co-localized with Ca^{2+} channels; granules in this pool experience much smaller, more global rises in cytosolic [Ca^{2+}] (at best several μM after buffered diffusion of Ca^{2+} from its entry sites), and display a much higher Ca^{2+} sensitivity. The HCSP, often small, is increased several to many-fold, by enhancing protein kinase A (PKA) and protein kinase C (PKC) activity as well as by increasing ambient [glucose];[12] it should particularly prominent under our experimental conditions of continuous application of forskolin and elevated bath [glucose]. Though traditionally tonic exocytosis has received scarce attention (reviewed in ref. 14), recent recordings from porcine β-cells suggest that it should contribute to exocytosis during intermittent PD lasting several seconds.[14] We have speculated that the differential Ca^{2+} sensitivity and spatial docking of granules of the IRP and HCSP may result from distinct isoforms of synaptotagmin.[14]

In emphasizing the presumed existence of two spatially distinct pools of granules, with widely different Ca^{2+} sensitivities, we assume elements of both of these pools exist under basal conditions. However, given the rapid rundown of both modes of exocytosis during intense electrical activity, it is likely that recruitment of granules is necessary to replenish and maintain both pools of granules during and after intense secretion. In a limited set of experiments (Appendix Fig. 3) we obtained data suggesting that the granule pools underlying both phasic and tonic exocytosis recovered from depletion over ~2 min, apparently along exponential time courses that were enhanced by elevated glucose. Also, our hypothesis does not preclude possible contributions that Ca^{2+}-dependent mobilization of granules or non-uniformity of Ca^{2+}

buffering might alter the latency of exocytosis after depolarization. Two possible contributory features merit consideration. First, during trains of APs or brief (25–50 ms) depolarizations applied at 1–4 Hz, often the probability of release is consistently higher in response to the second pulse than to the first pulse and further increases with subsequent depolarizations in the train (Fig. 3). Second, small amplitude depolarizations (say to -35 mV), which in themselves do not evoke exocytosis, nonetheless decrease the latency to first appearance of tonic QREs seen during an immediately subsequent depolarization (applied within 3 s) to voltages that support exocytosis (Misler S, Zhou Z and Dickey AS, unpublished data).

Two caveats about our experimental design worth further comment. *First,* while both our whole cell I_{Ca} and single channel data,[35] including evidence for lack of pre-pulse potentiation (Appendix Fig. 1A), support the notion that the I_{Ca} underlying exocytosis is an HVA Ca^{2+} current, likely of L-type, we have not performed detailed pharmacological dissection of Ca^{2+} currents. As both single-channel and whole-cell Ca^{2+} currents were difficult to suppress with a L-type Ca^{2+} channel antagonist, nifedipine and whole-cell Ca^{2+} current had two component of voltage-dependent inactivation,[19] we cannot rule out contributions made by P/Q or R-type Ca^{2+} currents, recently suggested to provide the bulk of the Ca^{2+} entry that is coupled to exocytosis in human β-cells.[36]

Second, while we have not used flash photolysis of caged Ca^{2+} to define the size of the IRP and HCSP, we have attempted indirect estimates of their sizes. We have tentatively estimated the maximum size of the IRP (or B_{max}), from the "run-down" of the C_m steps seen in response to the first two 100 or 200 ms depolarizations ($\Delta C_{m,1}$ and $\Delta C_{m,2}$, respectively) during a short train depolarizations applied at 1 Hz (i.e., $B_{max} = (\Delta C_{m,2} + \Delta C_{m,1})/(1 - \Delta C_{m,2}/\Delta C_{m,1})$.[37] In four experiments where (i) $\Delta C_{m,1}$ and $\Delta C_{m,2}$ displayed little or no creep component and (ii) sequentially evoked I_{Ca}s ran down by less than 5%, we estimated B_{max} to average 148 fF. Assuming an increase in C_m of 2 to 2.5 fF for the fusion of each dense core insulin-containing granule with the plasma membrane, this translates to ~60–80 insulin granules, or comparable to the size of the IRP in mouse β-cells as measured by flash photolysis of caged Ca^{2+}.[5-7] We roughly estimate the size of HCSP, from the total $C_{m,\ creep}$ recorded before exhaustion of ΔC_m and QREs during a short train and tentatively suggest that in our experimental conditions the size of the HCSP is at least three times that of the IRP.

In comparing the insulin secretion by radioimmunoassay with exocytosis single cell electrophysiology it is critical to note that the electrophysiological assays only require fusion pore formation and/or the diffusion of a highly mobile small molecule into the extracellular space. Hence they might overestimate the success of exocytotic events requiring full granule fusion and dispersion of the compact insulin crystal. In addition, even under conditions where both small and large molecules are successfully released, the kinetics of release of the large molecule might be significantly slower and its appearance in the bath delayed by up to several seconds. In principle, insulin sensing by amperometry would be an ideal technique for bridging the electrophysiological and immunological assays; however in practice, this technique is limited by measurement instability over the many minutes needed to measure biphasic insulin secretion. Two promising fluorescence imaging approaches to bridge the capacitance/amperometry and radioimmunoassay approaches involve the real-time monitoring of release of material known to be in the dense core of the insulin granule, such as GFP-tagged insulin (and/or C-peptide fragment) or Zn^{2+},[38-40] the latter reacting extracellularly with a fluorescent divalent cation chelator. The varying estimates of the efficiency of release of large granule contents, though not critical to our qualitative arguments, might be much more significant for any future quantitative reconciliation of results from the various approaches.

Finally, it is worthwhile attempting to reconcile our data and model with those of others. It is possible and even likely that the important physiological feature of biphasic insulin secretion may be based on several cellular mechanisms, which take on variable prominence in different species, as well as in a single species at different stages of development, under different conditions of innervation and aggregation and under varying exposure to paracrine (glucagon and somatostatin) and incretin (e.g., glucagon-like intestinal peptide-1 and acetylcholine) agents. Admittedly, in vitro canine β-cells display several features quite distinct from the standard mouse model, including Na^+_o-dependent APs, PDs, and the striking dependence of insulin secretion on the enhancement cytosolic [cAMP]. However, the former two features are shared with β-cells of other large, long-lived mammals including human and pig while minute-long PDs are seen in rat β-cells exposed to [glucose] > 10mM.[41a] Also incretins, which enhance insulin secretion by raising cytosolic [cAMP], are now recognized to support biphasic insulin secretion in situ from normal as well as β-cell-mass compromised islets in many species.[41] Furthermore, our data easily encompass previous ideas of two spatially distinct pools of granules, recently directly visualized,[11] contributing to biphasic insulin secretion, as well as the importance of recruitment of new and perhaps newly synthesized granules into the readily releasable pools directly maintaining SPIS.[4,42] Also there is no intrinsic contradiction between our data and that suggesting that SPIS can be mimicked in a K^+_{ATP} channel-independent manner by raising $[K^+]_o$ in the presence of a large concentration of diazoxide,[8] a condition that opens the latter channels and largely obliterates oscillations in $[Ca^{2+}]_i$. In canine β-cells examined in current clamp mode under perforated patch conditions, after metabolic inhibition by sodium azide (NaN_3, 1.3 mM) or treatment with diazoxide (DZ, at >150 μM), two conditions where K^+_{ATP} channels are massively open even in the presence of secretagogue concentrations of glucose, the membrane potential behaves as a K^+ selective electrode over a wide range of $[K^+]_o$.[35] In pilot experiments, in the face of 30 mM K^+ PSS, used to provoke K^+_{ATP} channel-independent rises in $[Ca^{2+}]_i$ and insulin secretion referred to above, canine β-cells exposed to 10 mM glucose and 250 μM diazoxide readily achieve PDs of ~-20 mV.[35] In principle, this should evoke exocytotic release of magnitude similar to those evoked by PDs generated by passage of depolarizing current or voltage clamp depolarization, provided DZ does not inhibit exocytosis as a side effect, an issue we have not specifically tested in whole canine islets or single β-cells. Furthermore, in principle, exocytosis evoked in this manner should

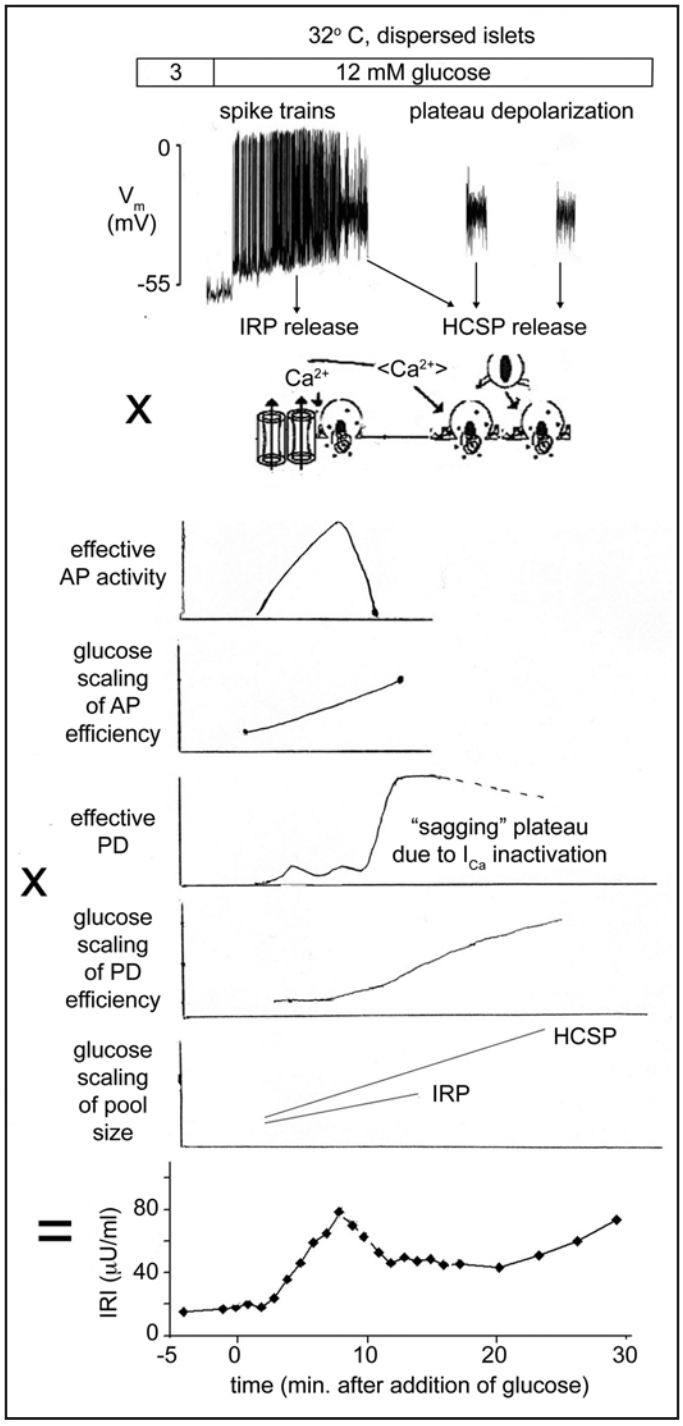

Figure 6. Summary hypothesis for coupling of spike train and plateau phases of electrical activity to insulin granule exocytosis from IRP and HCSP. Top trace shows tracing of early glucose-induced spike trains and later prolonged plateau depolarization seen on raising ambient [glucose] from 4 to 12 mm (reproduced from Fig. 1B). Second trace shows a schematic of how Ca^{2+} entry during the two phases of electrical activity contributes to exocytosis from granules of a low Ca^{2+} affinity pool (IRP) located very near voltage-dependent Ca^{2+} channels vs. from granules of a high Ca^{2+} affinity pool (HCSP) located at some distance from the voltage-dependent Ca^{2+} channels. Middle graphs show time courses of AP and plateau activities, including scaling of their efficiencies by elevated ambient [glucose] of 12 mM, as well as estimated changes in IRP and HCSP sizes achieved in raising [glucose] from 4 to 10–12 mM. Bottom trace depicts graph of time course of insulin secretion seen on raising ambient [glucose] from 4 to 12 mM (reproduced from Fig. 1A).

be enhanced by glucose metabolism either by increasing $[ATP]_i$ and/or decreasing $[ADP]_i$ or by producing another intracellular metabolic intermediate. However, the ability to mimic a phase of exocytosis under non-physiological conditions does not necessarily reveal physiological mechanisms.

Hence, the results we present here suggest that canine β-cells provide a relatively simple model for biphasic insulin secretion, features of which may be applicable to porcine, and perhaps other, β-cells, which display intermittent periods of PD with few superimposed APs during prolonged glucose exposure.[14] The model incorporates both the well-studied relationship of AP activity to exocytosis from IRP, likely prominent in FPIS of many species, and a novel relationship of PD to exocytosis from an HCSP, which we propose to be of varying prominence in SPIS by some species. The scaling of these features by glucose-induced and time-dependent changes in the sizes of IRP and HCSP may counteract subtle time-dependent changes in distinct patterns of electrical activity, such as decreases in AP frequency or sags in PD amplitude, and hence maintain and even enhance the distinct secretory phases (see summary Fig. 6). This new model is complementary to others of biphasic secretion. While de-emphasizing the potential importance of involvement of distinct Ca^{2+} channels in the two phases of secretion proposed by some,[10] it emphasizes the importance of docking of different pools of insulin granules, here proposed to be of distinctly different Ca^{2+} sensitivity and located at varying distance from Ca^{2+} entry channels, emphasized by others.[11]

Methods

Overall, the techniques used for single-cell electrophysiological, amperometric and fluorescence monitoring of single canine β-cells were virtually identical to those previously described in our recent studies of human and porcine β-cells.[14,22,23] The techniques used for preparation[24] and dispersion of islets, as well as for their perifusion in a filter chamber at 1 ml/min and radioimmunoassay of insulin release, were closely similar to those used in our previous studies of canine islets.[24,25]

The following specifics are worth noting. (i) Unless otherwise stated experiments were performed at 32°C and in the presence of 4 mM glucose and 10 μM forskolin in the bath to insure exocytosis under stable electrophysiological recording conditions and facilitate direct comparison of single cell electrical activity, exocytosis and insulin secretion under nearly identical conditions. As shown in our prior studies,[24,25] canine β-cells require enhancement of cytosolic [cAMP], via application of a membrane permeant cAMP derivative, a phosphodiesterase inhibitor, an activator of adenylyl cyclase, or glucagon, in order to respond to a rise in ambient [glucose] with biphasic insulin secretion or to Ca^{2+} entry induced by depolarization with measurable exocytosis (increase in C_m). 10 μM forskolin is near the minimum concentration needed to guarantee glucose-induced biphasic insulin secretion from canine islets at physiological temperature, while 5 μM forskolin was the minimum concentration needed to guarantee glucose-induced

depolarization and electrical activity in all single canine β-cells, nearly 40% of which did not respond to glucose but did respond to tolbutamide (30 μM) in the absence of forskolin.[24] In paired experiments performed at 24 or 28°C, increasing [forskolin] from 5 to 10 μM increased the rate of membrane depolarization by 2.3 +/- 0.4 fold (n = 6) (accompanied by faster decreases in background membrane conductance) and sped the time to start of plateau depolarization by 2.5 +/- 0.3 minutes (n = 5), but did not alter the basic pattern of biphasic electrical activity.[25]

(ii) Single-cell electrical recordings were made in the perforated-patch variant of the whole-cell recording configuration on cells, with baseline C_m > 6 pF (to maximize probability of recording from a β-cell[26]) bathed either in a physiological saline solution (PSS) (containing, in mM: 138 NaCl; 5.5 KCl; 2 $CaCl_2$; 1 $MgCl_2$; 3.0 glucose; 10^{-2} forskolin; and 20 HEPES buffer titrated with NaOH to pH 7.38), or in a partially tetraethylammonium-chloride-substituted saline solution (pTEAs-PSS), in which 40 mM NaCl was substituted mole-for-mole with TEA-Cl. Current-clamp recordings were made on cells bathed in PSS with the patch pipette filled with a high K^+ intracellular solution (K^+-IS), containing (in mM): 63.7 KCl; 28.35 K_2SO_4; 47.2 sucrose; 11.8 NaCl; 1 $MgCl_2$; and 20 HEPES titrated to pH 7.3 with KOH. Nystatin (at 250 μg ml^{-1}) was added to an aliquot of solution just proximal to the pipette tip. To evoke action potentials, cells maintained at ~-70 mV, through injection of a small current (<-5 pA), were rapidly depolarized by application of +5 to +10 pA current pulses of variable duration. Voltage-clamp recordings were performed with cells bathed pTEAs-PSS and the patch pipette filled with a Cs^+ intracellular solution (Cs^+-IS), where the K^+ content of the standard IS was substituted with Cs^+, conditions where voltage dependent Ca^{2+} currents (I_{Ca}) were likely to be easily quantified. The membrane potential (V_m) was stepped from a holding potential (V_{hold}) of -70 mV to the depolarized test potential (V_c) noted and evoked currents were leak subtracted using a standard p/4 protocol. As shown in Appendix Figure 1, the amplitudes of I_{Ca}s often remained stable over 15–20 minutes and showed no evidence of enhancement either by concentrations of glucose that evoke biphasic insulin secretion or by depolarizing pre-pulses.[27] Action potentials were simulated in the voltage-clamp mode by applying a multi-segment sequence of ramp depolarizations that together closely resemble averaged features of action potentials recorded in current-clamp mode in response to brief depolarizing pulses from a holding current of -2 to -5 pA. As shown in Appendix Figure 1C, in the presence of K^+ channel blockade, the resulting current traces show (i) an initial rapidly activating and inactivating current "spike", which is blocked by tetrodotoxin, followed by (ii) a more slowly activating and then deactivating current *hump*, enhanced by substitution of the $CaCl_2$ of the PSS (2 mM) with $BaCl_2$ (2 mM).

(iii) Membrane capacitance changes (ΔC_m) following membrane depolarization was usually estimated using an EPC-9 patch-clamp amplifier (Heka Electronic, Lambrecht, Germany) and an in-house developed, software-based, dual frequency lock-in detector (LID) developed as a set of extensions (XOP modules) of the numerical/graphics package Igor (Wavemetrics, Inc., Oregon, USA).[28] However, in selected experiments, where the responses to seconds-long depolarization were sought, the capacitance tracking feature of the EPC-9 software (*Captrack*) was used at a sampling frequency of 2 Hz (e.g. Fig. 4A).

(iv) Amperometry was performed on patch-clamped β-cells, previously loaded with serotonin (5-HT) and 5-hydroxytryptophan, each at incubation concentrations of 0.5 mM, using polypropylene insulated or electro-deposition paint-coated carbon fiber electrodes (ALA Scientific Instruments) that touched the surface of individual β-cells. The electrode was held at +650 mV using an EPC-7 amplifier (Heka, Germany). Amperometric data, filtered at 300 Hz using an 8 pole Bessel filter (Frequency Devices Haverhill, MA), were acquired simultaneously with electrophysiological data using the software package that runs the digital LID. Quantal release events (QREs) were tabulated with an interactive Igor-based program. A detailed characterization of QREs is presented Appendix Figure 2.

Note

Supplementary materials can be found at:
www.landesbioscience.com/supplement/MislerCHAN3-3-Sup.pdf

Acknowledgements

We thank (i) Dr. David Scharp for encouragement to undertake this project; (ii) the Human Islet Transplantation Laboratory, Washington University Medical Center, especially Barbara Olack and Carole Swanson, for the provision of islets; (iii) Yan-Fang Hu for preparation of the polypropylene-insulated carbon fiber electrodes used for amperometry; and (iv) Alon Friedman, Advanced Teacher Training Center at Shlomi, Israel for expert help with execution of several of the figures. This work was principally supported by grants from the National Institutes of Health (RO1-DK37380) and the Barnes-Jewish Hospital Research Foundation to Stanley Misler. Additionally, Adam S. Dickey was supported by a National Institutes of Health Medical Scientist Training Grant (5 T32 GM07281) to the University of Chicago.

References

1. Curry DL, Bennett LL, Grodsky GM. Dynamics of insulin secretion by the perfused rat pancreas. Endocrinology 1968; 83:572-84.
2. Nunemaker CS, Wasserman DH, McGuinness OP, Sweet IR, Teague JC, Satin LS. Insulin secretion in the conscious mouse is biphasic and pulsatile. Am J Physiol Endocrinol Metab 2006; 290:523-9.
3. Felig P, Bergman M. The endocrine pancreas: diabetes mellitus. In *Endocrinology and Metabolism* 3rd edition. Felig P, Baxter JD, Frohman LA, eds 1995; 1107-250.
4. Grodsky GM. A threshold distribution hypothesis for package storing of insulin and its mathematical modeling. J Clin Invest 1972; 51:2047-59.
5. Barg S, Ma X, Eliassson L, Galvanovskis J, Gopel SO, Obermuller S, et al. Fast exocytosis with few calcium channels in insulin-secreting mouse pancreatic β-cells. Biophys J 2001; 81:3308-23.
6. Barg S, Eliasson L, Renstrom E, Rorsman P. A subset of 50 secretory granules in close contact with L-type Ca^{2+} channels accounts for first-phase insulin secretion in mouse beta-cells. Diabetes 2002; 51:74-82.
7. Barg S, Olofsson CS, Schriever-Abeln J, Wendt A, Gebre-Medhin S, Renstrom E, Rorsman P. Delay between fusion pore opening and peptide release from large dense-core vesicles in neuroendocrine cells. Neuron 2002; 33:287-99.
8. Henquin J-C, Ishiyama N, Nenquin M, Ravier MA, Jonas J-C. Signals and pools underlying biphasic insulin secretion. Diabetes 2002; 51:60-7.
9. Gunawardana SC, Rocheleau JV, Head WS, Piston DW. Mechanisms of time-dependent potentiation of insulin release. Involvement of nitric oxide synthase. Diabetes 2006; 55:1029-33.
10. Jing X, Li D-Q, Olofsson C, Salehi A, Surve VV, Caballero J, et al. $Ca_V2.3$ calcium channels control second-phase insulin release. J Clin Invest 2005; 115:146-54.

11. Ohara-Imaizumi M, Fujiwara T, Nakamichi Y, Okamura T, Akimoto Y, Kawai J, et al. Image analysis reveals mechanistic difference between first- and second-phase insulin exocytosis. J Cell Biol 2007; 177:695-705.
12. Yang Y, Gillis KD. A highly Ca^{2+}-sensitive pool of granules is regulated by glucose and protein kinases in insulin-secreting INS-1 cells. J Gen Physiol 2004; 124:641-51.
13. Misler S, Barnett DW, Gillis KD. Update on Electrophysiology of Stimulus-Secretion Coupling in Human β Cells. *In* "*Retrospective on Perspectives in Diabetes*". R.P. Robertson, Alexandria, American Diabetes Association.
14. Misler S, Silva AM, Dickey AS, Barnett DW. Phasic and tonic modes of depolarization-exocytosis coupling in β-cells of porcine islets of Langerhans. Channels 2009; 3:101-9.
15. Gillis KD, Misler S. Single cell assays of exocytosis from pancreatic islet β cells. Pfluegers Arch 1992; 420:121-3.
16. Ammälä C, Eliassson L, Bokvist K, Larsson O, Ashcroft FM, Rorsman P. Exocytosis elicited by action potentials and voltage-clamp calcium currents in individual mouse pancreatic B-cells. J Physiol 1993; 472:655-88.
17. Smith PA, Duchen MR, Ashcroft FM. A fluorometric and amperometric study of calcium and secretion in isolated mouse pancreatic beta-cells. Pfluegers Arch 1995; 430:808-18.
18. Zhou Z, Misler S. Amperometric detection of quantal secretion from patch-clamped rat pancreatic β-cells. J Biol Chem 1996; 270:270-7.
19. Pressel DM, Misler S. Role of voltage-dependent ionic currents in coupling glucose stimulation to insulin secretion in canine islet β cells. J Membrane Biol 1991; 124:239-53.
20. Zhou Z, Misler S. Amperometric detection of quantal release of serotonin from canine pancreatic islet β-cells. Abstr Soc Neurosci 1995; 21:334.
21. Misler S, Dickey AS, Silva AM, Pressel DM, Barnett DW. Correlates of biphasic insulin secretion in single cell exocytosis by canine β-cells. Diabetes 2004; 53:393.
22. Misler S, Dickey A, Barnett DW. Maintenance of stimulus-secretion coupling and single beta-cell function in cryopreserved-thawed human islets of Langerhans. Pfluegers Arch 2005; 450:395-404.
23. Silva AM, Dickey AS, Barnett DW, Misler S. Ion channels underlying stimulus-exocytosis coupling and its cell-to-cell heterogeneity in β-cells of transplantable porcine islets of Langerhans. Channels 2009; 3:91-100.
24. Barnett DW, Pressel DM, Chern HT, Scharp DW, Misler S. cAMP-enhancing agents "permit" stimulus-secretion coupling in canine pancreatic islet β-cells. J Membrane Biol 1994; 138:113-20.
25. Barnett DW. Stimulus secretion coupling in canine and human pancreatic islet β-cells: studies using membrane capacitance as an assay of exocytosis. D.Sc. dissertation. Washington University, St. Louis 1995.
26. Göpel S, Kanno T, Barg S, Galvanovskis J, Rorsman P. Voltage-gated and resting membrane currents recorded from β-cells in intact mouse pancreatic islets. J Physiol 1999; 521:717-28.
27. Grynkiewicz G, Poenie M, Tsien RY. A new generation of Ca^{2+} indicators with greatly improved fluorescence properties. J Biol Chem 1985; 260:3440-50.
28. Barnett DW, Misler S. An optimized approach to membrane capacitance estimation using dual-frequency excitation. Biophys J 1997; 72:1641-58.
29. Pressel D, Misler S. Sodium channels contribute to action potential generation in canine and human pancreatic beta cells. J Membrane Bio 1990; 116:273-80.
30. Zawalich WA, Tesz GJ, Zawalich KC. Are 5-hydroxytrptamine-preloaded β-cells an appropriate physiological model for establishing that insulin stimulates insulin secretion? J Biol Chem 2001; 276:37120-3.
31. Augustine GJ, Neher E. Calcium requirements for secretion in bovine chromaffin cells. J Physiol 1992; 450:247-71.
32. Barnett DW, Misler S. Coupling of exocytosis to depolarization in rat pancreatic islet β-cells: effects of Ca^{2+}, Sr^{2+} and Ba^{2+}-containing extracellular solutions. Pfluegers Arch 2005; 430:593-5.
33. Silva AM, Liu-Gentry J, Dickey AS, Barnett DW, Misler S. α-Latrotoxin increases spontaneous and depolarization-evoked exocytosis from pancreatic islet β-cells. J Physiol 2005; 565:783-99.
34. Jones PM, Persuad SJ, Howell SL. Calcium-induced insulin secretion from electrically permeabilized islets. Biochem J 1992; 285:973-8.
35. Pressel DM. The role of ionic currents in coupling glucose stimulation to insulin secretion in canine pancreatic islet B cells. Doctor of Philosophy Dissertation, Graduate School of Arts and Science, Washington University in St. Louis 1993.
36. Braun M, Ramracheya R, Bengtsson M, Zhang Q, Karanauskaite J, Partridge C, et al. Voltage-gated ion channels in human pancreatic beta-cells: electrophysiological characterization and role in insulin secretion. Diabetes 2008; 57:1618-28.
37. Gillis KD, Moosner R, Neher E. Protein kinase C enhances exocytosis from chromaffin cells by increasing the size of the readily releasable pool of secretory granules. Neuron 1996; 16:1209-20.
38. Obermuller S, Linqvist A, Karanauskaite J, Galvanovski J, Rorsman P, Barg S. 2005 Selective nucleotide release from dense-core granules in insulin secreting cells. J Cell Sci 2005; 118:4271-82.
39. Michael DJ, Ritzel RA, Haataja L, Chow RH. Pancreatic β-cells secrete insulin in fast and slow release forms. Diabetes 2006; 55:600-7.
40. Qian W-J, Gee KR, Kennedy RT. Imaging of Zn^{2+} release from pancreatic *b*-cells at the level of single exocytotic events. Anal Chem 2003; 75:3468-75.
41. Holst JJ. The physiology of glucagon-like peptide-1. Physiol Rev 2007; 87:1409-39.

41a. Antunes CM, Salgado AP, Rosario LM, Santos RM. Differential patterns of glucose-induced electrical activity and intracellular calcium responses in single mouse and rat pancreatic islets. Diabetes 2000; 49:2028-38.

42. Lacy PE, Howell SL, Young DA, Fink CJ. A new hypothesis of insulin secretion. Nature 1968; 219:1177-80.
43. Chow RH, von Rueden L. Electrochemical detection of secretion from single cells. In Single Cell Recording 2nd ed. Sakmann B and Neher E, ed 1995.
44. Zhou Z, Misler S, Chow RH. Rapid fluctuations in transmitter release from single vesicles in bovine adrenal chromaffin cells. Biophysical J 1996; 70:1543-52.
45. Zhou Z, Misler S. Amperometric detection of stimulus-induced quantal release of catecholamines from cultured superior cervical ganglion neurons. Proc Natl Acad Sci USA 1995; 92:6938-42.